Journal of Korea Multimedia Society Vol. 22, No. 12, December 2019(pp. 1396-1403)
https://doi.org/10.9717/kmms.2019.22.12.1396

Adaptive Gaussian Model Based Ground Clutter Mitigation Method for Wind Profiler

Sanghun Lim†, Shaik Allabakash††, Bong-Joo Jang†††

ABSTRACT

The radar wind profiler data contaminates with various non-atmospheric components that produce errors in moments and wind velocity estimations. This study implemented an adaptive Gaussian model to detect and remove the clutter from the radar return. This model includes DC filtering, ground clutter recognition, Gaussian fitting, and cost function to mitigate the clutter component. The adaptive model tested for the various types of clutter components and found that it is effective in clutter removal process. It is also applied for the both time series and spectrum datasets. The moments estimated using this method are compared with those derived using conventional DC-filtering clutter removal method. The comparisons show that the proposed method effectively removes the clutter and produce reliable moments.

Key words: Wind Profiler, Adaptive Gaussian Method, Ground Clutter Mitigation

1. INTRODUCTION

In radar wind profiler (RWP), returned signals consist of clear-air signal, clutter and noise. To retrieve the characteristics of desired clear-air signals, the returned signals need signal processing, which can distinguish different echoes present in the signal. Clutter is the totality of undesired echoes and interfering signals. Clutter can be categorized as intermittent, ground and hydrometeor clutter. Intermittent clutter can be caused by bird, insects or airplane, where hydrometeor clutter is from precipitation such as rain, hail or snow. Ground clutter is usually produced by scatter from building, trees, or wind turbines.

Many signal processing techniques developed to remove the clutter contamination from the radar and wind profiler data[1-5]. The clutter suppression fence uses to prevent the interference entering into the radar return[1]. The ground clutter detects using the clear air echo as the reference [5]. The conventional DC/fixed clutter removal technique in the time domain is based on the mean value of complex signal (I+jQ) subtraction from it (I+jQ)[6,7]. This method removes only the DC point (zero Doppler velocity point on the Doppler velocity axis) and it is ineffective to remove the ground clutter. In the frequency domain, three-point or five-point DC removal uses to mitigate the ground clutter[8]. This technique has the limitations i) if the clear air signal overlapped/close to the DC point, it may remove the clear air part along with the clutter, ii) if the clutter width is large (occupy more than three-data points), it is not

※ Corresponding Author : Sanghun Lim, Address: (10223) 283, Goyangdae-Ro, Ilsanseo-Gu, Goyang-Si, Gyeonggi-Do Korea, TEL : +82-31-910-0373, FAX : +82-31-910-0100, E-mail : slim@kict.re.kr
Receipt date : Dec. 4, 2019, Revision date : Dec. 3, 2019
Approval date : Dec. 10, 2019
† Dept. of Land, Water and Environment Research, Korea Institute of Civil Engineering and Building Technology
†† Dept. of Land, Water and Environment Research, Korea Institute of Civil Engineering and Building Technology (E-mail : shaik@kict.re.kr)
††† Dept. of Land, Water and Environment Research, Korea Institute of Civil Engineering and Building Technology (E-mail : roachjbj@kict.re.kr)
※ This research was supported by Korea Institute of Civil Engineering and Building Technology Research Project (Smart Vehicle Driving Assistance Technology Based on Pedestrian Tracking and Behavior Analysis)

suitable to remove the total clutter.

In this study, ground clutter removal will be dealt only with. Currently, the conventional method adopts DC filtering and linear interpolation at DC point for ground clutter cancellation. In spite of convenience of algorithm implementation, this method can over-cancel at DC point and under/over-cancel at neighbor points of DC point. On the assumption of homogeneous and isotropic turbulence in the resolution volume, velocity of clear-air echoes can be distributed as Gaussian. The Gaussian Model Adaptive Processing (GMAP) filter was introduced by Siggia and Passarelli [9], which used a Gaussian clutter model to remove ground clutter over a variable number of spectral components. Due to the dynamic range/width of the GMAP filter, it can able to remove the clutter efficiently. GMAP was originally developed for weather radar such as NEXRAD. In this research, GMAP will be tested and modified for RWP.

2. GROUND CLUTTER MITIGATION SYSTEM USING GAUSSIAN MODEL

The Gaussian model technique for ground clutter suppression starts with three major assumptions as

- The returned echoes consist of clear-air signals, ground clutter and noise. It means that before ground clutter suppression intermittent clutter impact or other impact such as ring effect need to be separated or minimized.
- Ground clutters are distributed approximately as Gaussian with zero mean. Clear-air echoes are also distributed approximately as Gaussian.
- The spectrum width of the clear-air signal is greater than that of the ground clutter.

Based on these assumptions, the algorithm remove ground clutter region with assumed clutter width or calculated clutter width and then interpolates iteratively over the removed ground clutter region. The ground clutter suppression system using Gaussian model consists of three steps: Decision of ground clutter region and clear-air echo region, adaptive Gaussian model algorithm and estimation of moments. The block diagram of the system is shown in Fig. 1.

The block of "Find dwell signal boundary" plays a role of defining signal boundary for all rays of one dwell time. A dwell signal boundary can be detected by averaging of all ray spectral data and finding the signal peak with widest spectral width.

2.1 Decision of ground clutter region and clear-air region

The purpose of this step is to perform ground clutter suppression effectively. It means that ground clutter cancellation algorithm works only in case that ground clutter and clear-air region are overlapped. If ground clutter and clear-air region are not overlapped, ground clutter region can just removed and replaced as noise level.

For time series data input, ground clutter region can be decided by comparing the power spectrum without DC-filtering and the DC filtered power spectrum of returned signal. In this study, if the power spectrum data without DC-filtering are greater than the DC filtered power spectrum data within boundary of ±1 m/s, the region is decided as ground clutter. Fig. 2 shows an example of

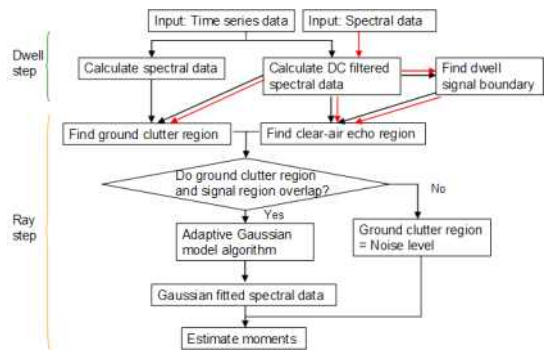

Fig. 1. Block diagram of ground clutter suppression system. In dwell step, black flow lines indicate for input of time series data and red lines are for input of spectral data.

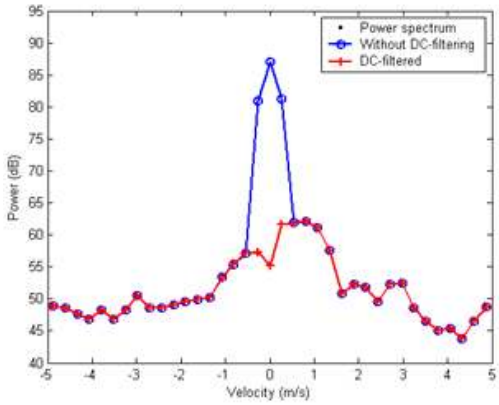

Fig. 2. An example of ground clutter region detection using time series data.

ground clutter region detection using time series data.

For spectral data input, the ground clutter region detection algorithm is more complicate. The block diagram of detecting ground clutter region is shown in Fig. 3. Using linearly-interpolated spectral data, first a signal peak near DC-point that is within ±1 m/s boundary is selected. Next, initial ground clutter region is chosen by checking the gradients from the selected peak. After finding initial ground clutter region, spectral data are interpolated linearly for initial ground clutter region. From the interpolated data, we can find clear-air echo region and check whether these clear-air echoes

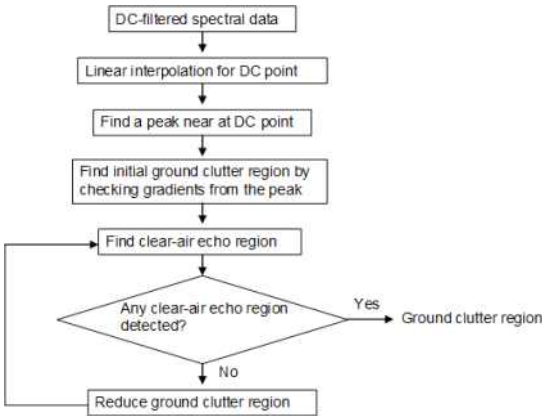

Fig. 3. The block diagram of detection of ground clutter region in case of spectral data input.

has enough spectrum width (greater than 1 m/s) and power level (greater than maximum noise level). If the detected clear-air echo region does not satisfy these conditions, the detected ground clutter region is reduced by removing most left and right points. The process is repeated until good clear-air echo region is found. If the process is failed to detect ground clutter region, the points that the magnitude of velocity are less than 0.6 m/s are assumed as ground clutter region. This assumption is reasonable for WP. Fig. 4 shows an example of ground clutter region detection using DC-filtered spectral data.

To decide clear-air region, first the ground clutter region is interpolated linearly by using values of the nearest neighbor points and linearly interpolated power spectrum is smoothed by three-points moving average. Next, a nearest peak from ground clutter region is select as clear-air peak for Gaussian model fitting. The total clear-air region is decided from selected peak points and gradient of smoothed power spectrum.

2.2 Adaptive Gaussian model algorithm

Gaussian model that represents clear-air echoes can be obtained by iterative approach. This procedure starts from the power spectrum interpolated linearly for removed ground clutter. At first iteration, first moments (P1,m1 and s1) are calculated

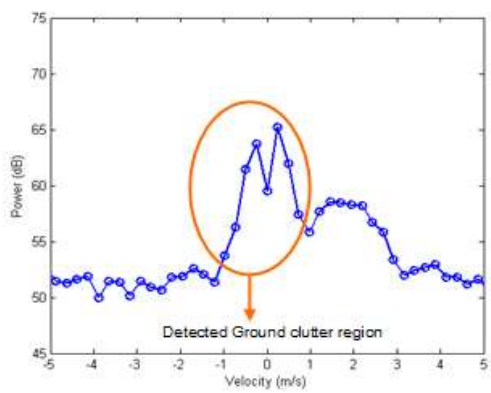

Fig. 4. An example of ground clutter region detection using DC-filtered spectral data.

from linear interpolated power spectrum and then a Gaussian model is constructed from calculated moments. Next, ground clutter points are replaced by constructed Gaussian model. To find an optimal Gaussian model, the only signal region points of constructed Gaussian model and original power spectrum are compared. Cost function for comparison process is defined as

$$C_i = \sum_k |S_{Gi}(k) - S(k)| \tag{1}$$

where $S_{Gi}(k)$ and $S(k)$ indicate constructed Gaussian model and original power spectrum respectively and k is only signal region index. These steps are repeated until cost function reaches minimum. The block diagram of adaptive Gaussian model algorithm is shown in Fig. 5.

2.3 Estimation of moments

The normalized spectral moment can be defined as,

$$\mu_k(S(f)) = \frac{\int_{-\infty}^{\infty} f^k S(f) df}{\int_{-\infty}^{\infty} S(f) df} \tag{2}$$

From (2), mean power is calculated by zero moment (k=0) where mean velocity is computed by first moment (k=1).

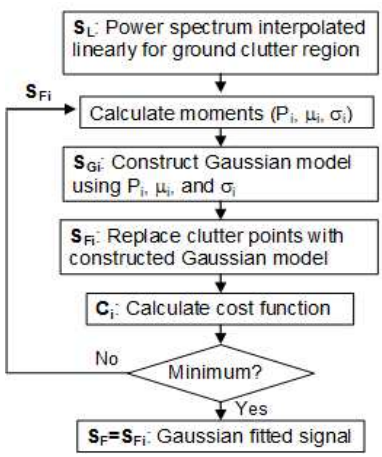

Fig. 5. Block diagram of adaptive Gaussian model algorithm.

The spectral width is defined as,

$$\sigma(S(f)) = [\mu_2(S(f)) - \mu_1^2(S(f))]^{1/2} \tag{3}$$

2.4 Calculation of noise level

Two methods of noise level calculation are used. One is named as linear-line threshold method and the other is subspace method. To find mean noise level and maximum noise level the linear-line threshold method is used firstly. If this method failed, then subspace method is used. If there is ring effect or intermittent clutter contamination, linear-line threshold method can failed. For linear-line threshold method, first the spectral data are sorted. Using low-half of sorted spectral data, linearly-fitted line is calculated and the line is extended to high-half. In high-half of sorted data, maximum noise level is decided as the maximum value of power less than linearly-fitted line. Mean noise level can be calculated by averaging the values less than maximum noise level. The Fig. 6 shows an example of linear-line threshold method.

The subspace method divides to several subspaces and calculates mean and standard deviation of each subspace. Next, mean noise level is decided as the mean noise level at subspace that has the minimal value of the multiplication of mean and standard deviation. Maximum noise level is calculated by adding mean noise level and standard deviation.

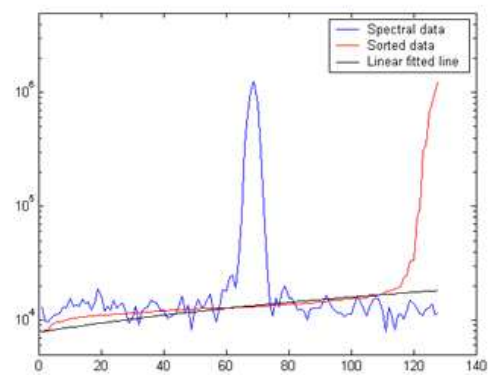

Fig. 6. An example of noise level calculation for linear-line threshold method.

3. CASE STUDY

The adaptive Gaussian model algorithm is tested extensively for various scenarios. Here case studies for two different RWP are presented. The data used for test are from YUM and PIT RWP. The followings show the results of testing.

3.1 Case 1: YUM; Apr. 23, 2005 000022 UTC

First test case data is from YUM RWP, which operated at AZ. 335 and El. 90. Fig. 7 shows the results of test for case 1. Left panel shows the contour plot by adaptive Gaussian model algorithm and right panel is by conventional DC-filtering method (LAP-XM). The red lines indicate mean velocity and spectrum width of adaptive Gaussian model algorithm and black lines are those of LAP-XM. Fig. 8 shows a comparison of both methods at 0.18 km corresponding to Fig. 7. Green line is from LAP-XM and black line indicates an optimal Gaussian model. Red line indicates the result from adaptive Gaussian model algorithm, which ground clutter region of original power spectrum is replaced with the optimal Gaussian model. From the results of Fig. 7 and 8, we can see that the adaptive Gaussian model algorithm works well. The adaptive Gaussian model algorithm can compensate over-cancelled ground clutter by DC-filtering.

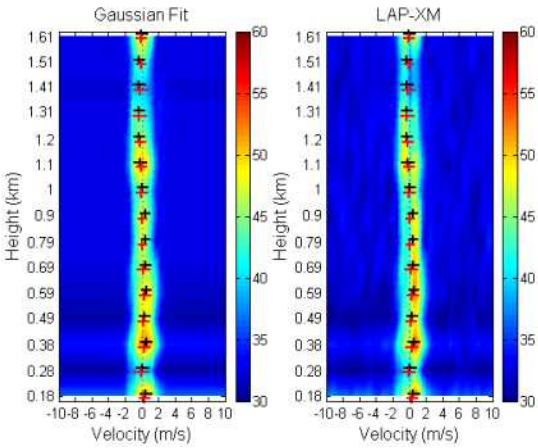

Fig. 7. Contour plot of stacked Doppler spectra (left panel -adaptive Gaussian model algorithm, right panel -LAP-XM, red line - moments from adaptive Gaussian model algorithm, black line - moments from LAP-XM).

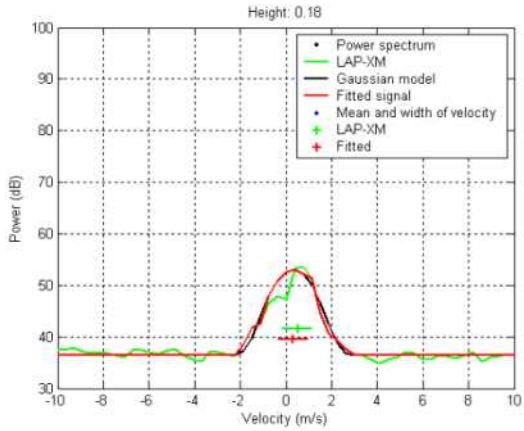

Fig. 8. A comparison of adaptive Gaussian model algorithm and LAP-XM at 0.18 km of height corresponding to Fig. 7.

3.2 Case 2: PIT; Jul. 31, 2004

Second test case data is from PIT RWP. Here two different elevation cases are tested. One is at AZ. 260 - EL. 90. The other is at AZ. 260 - EL. 66.4.

3.2.1 000011 UTC

This test data is from at AZ. 260 and El. 90. Fig. 9 and 10 show comparison of adaptive Gaussian model algorithm and LAP-XM. The stacked spectra shown in Fig. 9, while a single spectrum at 0.34 km height given in Fig. 10. It is clearly observed that the LAP-XM (right panel of Fig. 9) shows the high signal power near zero Doppler point at lower heights represents the ground clutter. Thus, the LAP-XM is unable to remove the total contamination, accordingly error presents in the mean Doppler velocity and spectrum width measurements. On the other hand, adaptive Gaussian model (left panel of Fig. 9) shows the low signal power below 0.6 km height compared to LAP-XM, which indicates the mitigation of the ground clutter. Therefore, the calculated moments and spectrum

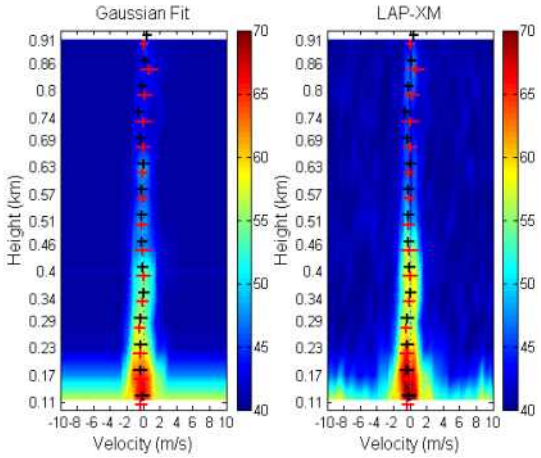

Fig. 9. Contour plot of stacked Doppler spectra (left panel -adaptive Gaussian model algorithm, right panel -LAP-XM, red line - moments from adaptive Gaussian model algorithm, black line - moments from LAP-XM).

width were also reliable. To describe the efficiency of the algorithm, we used a single spectrum corresponds to 0.34 km height is shown in Fig. 10. The green and red color lines illustrate the LAP-XM and adaptive Gaussian model, respectively. The LAP-XM shows mean Doppler at zero velocity point that corresponds to clutter peak; while the adaptive Gaussian model removes the clutter peak and presents the true Doppler velocity.

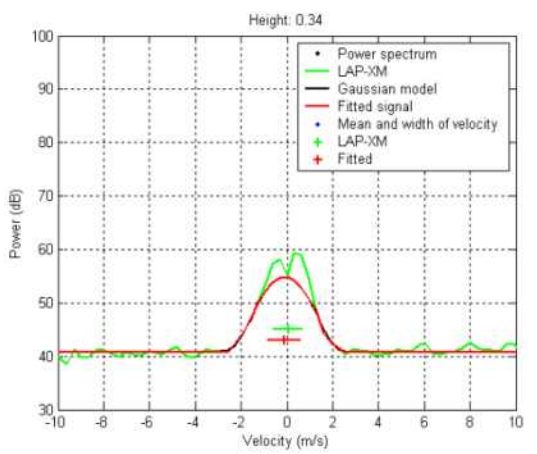

Fig. 10. A comparison of adaptive Gaussian model algorithm and LAP-XM at 0.34 km of height corresponding to Fig. 9.

3.2.2 000030 UTC

This test data is from at AZ. 260 and El. 66.4. Fig. 11 and 12 show comparison of adaptive Gaussian model algorithm and LAP-XM. This case shows the clutter and clear air signal both with equal powers and the lower heights present multiple noise/clutter peaks. Fig. 11 right panel shows the LAP-XM derived spectra with moments. It is clearly shows that the ground clutter strong illustrated by high powers and also exhibits noise at lower heights that produced error in moments. The Gaussian model derived spectra is shown in left panel of Fig. 11. This model removes the non-atmospheric components (clutter and noise) effectively. The expanded spectrum at 0.51 km height presented in Fig. 12. From this Figure, it can be observed that the proposed method (red line) produced reliable Doppler velocity and Doppler width than that of the LAP-XM (green line).

4. SUMMARY AND DISCUSSION

In this study, adaptive Gaussian model algorithm is introduced for RWP. The algorithm is similar to GMAP that developed by Siggia and

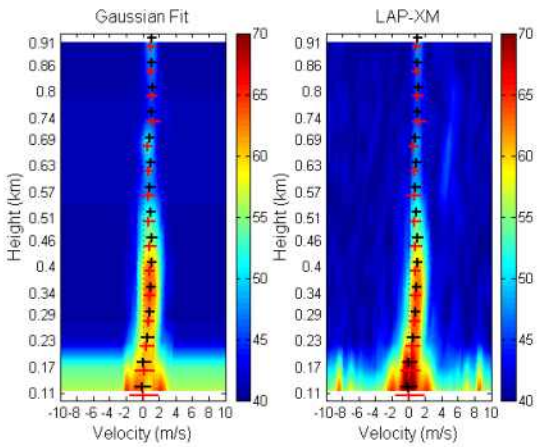

Fig. 11. Contour plot of stacked Doppler spectra (left panel -adaptive Gaussian model algorithm, right panel -LAP-XM, blue line - moments from adaptive Gaussian model algorithm, black line - moments from LAP-XM).

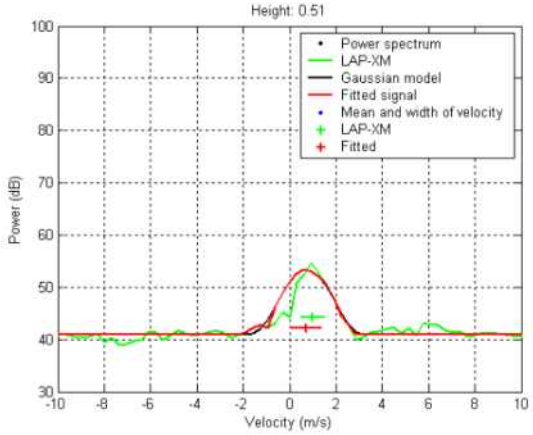

Fig. 12. A comparison of adaptive Gaussian model algorithm and LAP-XM at 0.51 km of height corresponding to Fig. 11.

Passarelli[9]. However, there are some differences. The new adaptive Gaussian model algorithm proposed here uses power spectrum that interpolated linearly for ground clutter region as input of the algorithm where GMAP used power spectrum removed ground clutter region. The most important feature is that the suggested algorithm uses the cost function, which contributes to obtain more accurate optimal Gaussian model. Another feature of suggested algorithm is detection algorithm of ground clutter region. This algorithm can detect varying ground clutter region. The proposed algorithm is tested for two different RWP with different angle and mode. We applied the algorithm for the various types of clutter components and observed that the proposed method is adequately removing the contamination than that of conventional DC-filtering method. The results of test show that the algorithm works effectively and produce reliable moments.

REFERENCE

[1] C.A. Russell and J.R. Jordan, "Portable Clutter Fence for UHF Eind Profiling Radar," *Preprints 7th Symposium on Meteorological Observations and Instrumentations,* pp. J152-J156, 1991.

[2] T. Sato and R.F. Woodman, "Spectral Parameter Estimation of CAT Radar Echoes in the Presence of Fading Clutter," *Radio Science*, Vol. 17, No. 4, pp. 817-826, 1982.

[3] A.C. Riddle and W.M. Angevine, "Ground Clutter Removal from Profiler Spectra," *Proceeding of 5th Workshop of Technical and Scientific Aspects of MST Radar, URSI/SCOSTEP*, pp. 418-420, 1992.

[4] B.-J. Jang, S. Lim, W. Kim, and H. Noh, "DCT and DWT based Damaged Weather Radar Image Retrieval," *Journal of Korea Multimedia Society*, Vol 20, No. 2, pp. 153-162, 2017.

[5] R.E. Passarelli, "Ground Clutter Rejection in the Frequency Domain," *Preprints 20th Conference On Radar Meteorology,* pp. 295-300, 1981.

[6] R.G. Strauch, D.A. Merritt, K.P. Moran, K.B. Earnshaw, and D.V. De Kamp, "The Colorado Wind-profiling Network," *Journal of Atmospheric and Oceanic Technology*, Vol. 1, No. 1, pp. 37-49, 1984.

[7] D.A. Carter, K.S. Gage, W.L. Ecklund, and W.M. Angevine, "Developments in UHF Lower Tropospheric Wind Profiling at NOAA's Aeronomy Laboratory," *Radio Science,* Vol. 30, No. 4, pp. 977-1002, 1995.

[8] M.F. Barth, R.B. Chadwick, and D.W. Van De Kamp, "Data Processing Algorithms Used by NOAA's Wind Profiler Demonstration Network," *Annales Geophysicae,* Vol. 12, No. 6, pp. 518-528, 1994.

[9] A.D. Siggia and R.E. Passarelli, "Gaussian Model Adaptive Processing (GMAP) for Improved Ground Clutter Cancellation and Moment Calculation," *Proceeding of Third European Conference on Radar in Meteorology and Hydrology*, pp. 67-73, 2004.

Sanghun Lim

received the Ph.D. degree in Electrical Engineering from the Colorado State University in 2006. Since then he had carried out various researches in radar meteorology and hydrology as research scientist of Colorado State University and NOAA/CIRA. Currently, he is a research fellow at Korea Institute of Civil Engineering and Building Technology and pursuing development of advanced weather observation systems and radar remote sensing using dual-polarization radars and automotive sensors.

S. Allabakash

received Ph.D. degree in atmospheric Physics from Sri Venkatewsara University, Tirupati, India, in 2016. Currently, he is a Post-Doctoral fellow with the Korea Institute of Civil Engineering and Building Technology, South Korea. His research interests include cloud microphysics and precipitation study, dynamics of atmospheric boundary layer, radar meteorology, and radar signal processing.

Bong-Joo Jang

received his B.S. and M.S. degrees in electronic engineering from Busan University of Foreign Studies, and Ph.D. degree in information security from Pukyong National University in 2002, 2004 and 2013 respectively. He visited Colorado State University in USA at 2011 - 2012 with visiting scholar. He is currently a Senior Researcher in Korea Institute of Civil Engineering and Building Technology. His research interests include multimedia data compression and digital image/video/vector processing, and now his major interests are weather radar system, radar signal processing and weather forecasting.